J Fluoresc (2007) 17:749–757
DOI 10.1007/s10895-007-0186-0

ORIGINAL PAPER

Single Molecule Spectroscopy of Poly 3-octyl-thiophene (P3OT)

Rodrigo E. Palacios · Paul F. Barbara

Received: 2 February 2007 / Accepted: 19 March 2007 / Published online: 25 April 2007

Abstract We report on the spectroscopy of isolated chains of P3OT, in a highly dilute solution in the inert polymer host poly(methyl–methacrylate) (PMMA). This environment permits a detailed analysis of emission transitions in the 1.9–2.2 eV range by suppressing the formation of the lowest emitting-energy aggregated form of P3OT. Herein it is observed that the 1.9–2.2 eV band is in fact split into low (red) and high (blue) energy forms in a highly analogous situation to that found for the conjugated polymer MEH-PPV. Another focus of this work is an investigation of the interaction of singlet and triplet excitons in P3OT. The results indicate that, like in MEH-PPV, triplet excitons are highly efficient fluorescence quenchers for P3OT, strongly quenching the fluorescence of P3OT under even relatively low excitation intensities.

Keywords Single molecule spectroscopy · Poly 3-alkyl-thiophene (P3AT) · Poly-3-octyl-thiophene (P3OT) · Bimodal emission · Singlet–triplet interaction

R. E. Palacios · P. F. Barbara
Department of Chemistry and Biochemistry and the Center for Nano- and Molecular Science and Technology, University of Texas, Austin, TX 78712, USA

R. E. Palacios
e-mail: rodpalacios@mail.utexas.edu

P. F. Barbara (✉)
1 University Station, A5500, Austin, TX 78712, USA
e-mail: p.barbara@mail.utexas.edu

Introduction

The poly-3-alkyl-thiophene) (P3AT) "family" of conjugated polymers has been extensively studied due to their importance in the fabrication of organic light-emitting diodes (OLEDs) [1–5], thin film transistors [6, 7], and photovoltaic cells [8–11]. An adequate knowledge of the electronic structure and excited state dynamics of this class of polymers is essential for understanding the mechanisms that govern device performance. Despite the considerable amount of research done on P3AT derivatives, many key aspects of their electronic structure and spectroscopy remain poorly understood. Thin-films morphologies of compounds in the P3AT class are highly heterogeneous leading to a large range of electronic transition energies. Multiple types of excited states are present in solution and pure films with an extraordinary large spread of vibronic origin transition energies, i.e. 1.9–2.5 eV. Although these states are not understood in detail, evidence suggests that various factors are responsible for the large shifts in the transition energies, including the specific conformation of the polymer chain, chain–chain aggregation, and the formation of crystalline phases [12–22].

The spectroscopy of P3AT conjugated polymers is analogous in many respects to that for the more widely investigated poly-phenylene-vinylenes, especially the prototypical poly[2-methoxy, 5-(2′-ethylhexyloxy)-p-phenylenevinylene] (MEH-PPV). Single molecule spectroscopy (SMS) of isolated polymer chains of MEH-PPV has offered a unique window on the effect of morphology on the spectroscopy of this polymer [23]. In addition, time-resolved SMS methods have been used to investigate the *spectroscopic dynamics* of MEH-PPV, leading to an unprecedented understanding of the interaction of triplet and singlet excitons in MEH-PPV [24, 25].

This paper describes the first single molecule spectroscopy of a P3AT conjugated polymer. Isolated chains of poly-3-octyl-thiophene (P3OT), in an inert polymer host, are studied using both time and frequency resolved techniques. Such an environment completely inhibits the formation of the lowest energy aggregated form of P3OT (with multiple peaks in the 1.3–1.8 eV range) and allows for a detailed analysis of emission in the 1.9–2.2 eV range. In this work it is observed that this band is in fact split into low (red) and high (blue) energy forms in a highly analogous situation to that found for MEH-PPV [26–29]. Another focus of this work is an investigation of the interaction of singlet and triplet excitons in P3OT. The results indicate that, like in MEH-PPV, triplet excitons are highly efficient fluorescence quenchers for P3OT, strongly quenching the fluorescence of the P3OT under even relatively low excitation intensities.

Experimental section

Ultra dilute thin-film samples of P3OT (Aldrich, MW= 142 kDa, regioregularity >98.5% head-to-tail) were prepared according to a reported procedure. [29] Typically, samples were diluted (10^{-9} M) in a solution of poly (methyl–methacrylate) (PMMA, Aldrich MW=95 kDa) in toluene (3%w/w) and spin-cast onto glass coverslips to yield films of approximately 100-nm thickness. Samples were then coated with either gold or aluminum (~200 nm) to prevent oxygen and water from diffusing into the PMMA layer. For nanoparticle samples a 300 nm-thick polyvinyl alcohol (PVA, Aldrich) layer imbedded with P3OT nanoparticles was used. Aggregates were prepared by a reprecipitation technique as described elsewhere [30–32]. Single molecules and nanoparticles were excited with the 488 nm line of an argon ion laser and images and spectra were obtained from a confocal scanning microscope apparatus described elsewhere [33]. Excitation intensities were approximately 50 W/cm^2. For time-resolved experiments fluorescence transients were acquired using a previously described setup [24]. Briefly, the transient signal was recorded with a multichannel scalar (MCS) that was synchronized to a sequence of excitation pulses. The sequence of excitation pulses was derived from the output of an argon ion laser (488 nm) that was intensity-modulated by an acoustic optical modulator.

Results and discussion

Ensemble spectra

It is well known that the UV-visible emission and absorption spectroscopy of P3OT is extraordinarily broad and complex due to a combination of intricate factors; some of which are highly dependent on the physical state of the sample. Several factors can strongly influence the spectra, including the solvent, temperature, and concentration for solutions; and the processing conditions for pure films. Figure 1 summarizes the absorption and emission spectra of P3OT in different environments, using data from this and other laboratories. Besides the usual vibronic splitting due to molecular vibrations (see for example the peaks labeled with "V" in Fig. 1) the emission spectra are also split due to shifts in the vibronic origin of the π–π* transition of P3OT by the local single-chain conformation and chain–chain interactions.

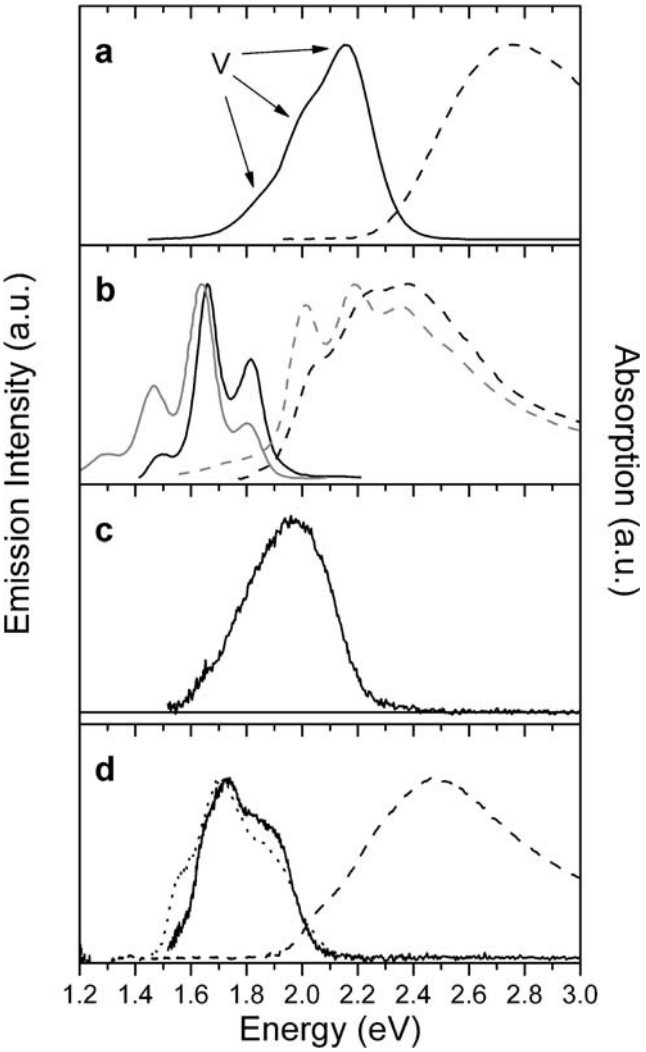

Fig. 1 (**a–d**) Absorption and emission spectra of P3OT in different environments. (**a**) Chloroform solution absorption (*dashed line*) and emission (*solid line*). (**b**) Room temperature pure film absorption (*dashed line*) and emission (*solid line*), adapted from references [41] and [18]. Low temperature (77 K) pure film absorption (dashed grey line) and emission (*solid grey line*), adapted from reference [15]. (**c**) Ensemble emission of single molecule spectra in PMMA matrix. (**d**) Absorption (*dashed line*) and emission (*dotted-dashed line*) spectra of nanoparticles suspended in water, and ensemble emission of single nanoparticles in PVA matrix (*solid line*)

The simplest situation is a dilute P3OT solution in a "good" solvent for which the intra-chain and inter-chain interactions are significantly suppressed due to favorable solvent–solute interactions (Fig. 1a, solid and dashed lines). The emission and absorption of conjugated polymers in this case is similar to those observed for similarly structured oligomers in solution, demonstrating that the long polymer chain has quasi-localized "π–π* chromophores" with a distribution of conjugation lengths in the range of 9–13 repeat units for the case of the regioregular P3OT used in this work [34–38]. The actual chain length (~720 repeat units) is much longer than the conjugation length allowing for multiple chromophores.

It should be emphasized that the peak of the emission spectra (2.18 eV) in a good solvent is at much lower energy than the absorption peak (2.75 eV) indicating that the most probable conjugation length for the emission is much longer than the most probable conjugation length for absorption. For the conjugated polymer MEH-PPV, an analogous observation was assigned to highly efficient inter-chain intramolecular energy transfer from regions of shorter conjugation length to less plentiful longer regions along the polymer chain. However, the observation that both the emission and absorption spectra of P3OT in solution in a good solvent are similar in shape to the corresponding ones for an oligomer composed of ~11 thiophene units suggests that excited torsional relaxation in these environments may be another factor responsible for the much longer conjugation length in emission for P3OT.

In order to organize these set of complex results we denote the short and long conjugation length electronic transitions as Type I and Type II chromophores respectively, see Table 1. The relatively sharp Type II emission is consistent with the general results for conjugated polymers that, even for planar systems, the transition energy approaches a minimum value for a large number of repeat units due to electron correlation effects. In contrast for short chains, there is a strong dependence of the transition energy on the number of repeat units due to the 1D spatial confinement of the electronic wave function.

It is interesting that the spectroscopy of P3OT reveals that the conjugation length distribution significantly shifts toward longer values as the solvent quality is decreased. This is evidence that the chain folding and perhaps small amounts of chain–chain aggregation induce a more planar conformation *in the ground state of P3OT* due to chain–chain packing forces, increasing the number of Type II chromophores in the ground state of P3OT.

The effect of chain–chain interaction and polymer morphology on the spectroscopy of P3OT is especially apparent in the spectroscopy of well ordered thin-films (Fig. 1b). At room temperature, emission peaks at 1.82 and 1.66 eV are observed in these films, and have been assigned to two distinct crystalline phases with different inter-chain stacking distances, on the basis of X-ray diffraction, solid state NMR, and powder emission studies [20–22]. These results suggest that the different spectral positions of the emission peaks corresponding to these two phases is related to different inter-chain interactions rather than intra-chain properties. At low temperatures (~77 K), the spectra of well-ordered films show a small red shift and sharpening of the spectral features compared to the corresponding spectra at room temperature. In general, the multiple absorption and emission peaks of the films are equally spaced and this is especially clear in the spectra of the film at low temperature (Fig. 1b). These equally spaced frequency intervals are indicative of vibronic transitions corresponding to the same chromophoric species. In particular, the observed ~0.18 eV (1450 cm^{-1}) interval might be assigned to C–C stretching modes in the thiophene ring [39]. Regardless of the interpretation about the origin of the regular frequency intervals, it is clear that the multiple transitions in the 1.9–1.2 eV emission range are a consequence of interchain interactions, we denote them collectively as Type III chromophores.

Herein we examine the spectroscopy of single isolated polymer chains of P3OT in a PMMA matrix. The spin-coating approach used to prepare these samples effectively suppresses chain–chain interaction. The ensemble spectrum for these samples (Fig. 1c) reveals a broad emission with a peak that is lower in energy than the peak emission in the good solvent chloroform but higher in energy than the aggregate type emission. The broad emission indicates a large distribution of emission energies for the individual P3OT chains in the PMMA environment. The P3OT emission in this case can be assigned exclusively to Type II emission. The observed broadening and red-shift can be explained in terms of chain packing effects that split the

Table 1 Summary of optical transition energies for P3OT

Chromophore type	Peak absorption (eV)	Peak emission (eV)
I (Short conjugation length)	2.75[a]	–
II (Long conjugation length)	–	2.10–2.15 (A) 1.95–2.00 (B)
III (Aggregate type)[b]	2.01, 2.19, 2.37. (*R*) 2.05, 2.22, 2.39. (*L*)	1.48, 1.65, 1.82. (*R*) 1.3, 1.47, 1.64, 1.81. (*L*)

[a]Broad and structureless peak.
[b]Position of the multiple peaks observed at room temperature (*R*) and at 77 K (*L*).

Type II emission into two sub-types, IIA and IIB, in analogy to the red and blue sites recently reported for MEH-PPV [26–29].

Figure 1d shows a P3OT sample preparation that is intermediate between the isolated polymer chains and a pure thin film. Here a colloidal solution of P3OT nanoparticles (each comprised of >50 chains) in water (Fig. 1d, dotted line) exhibits Type III emission with emission peaks at ~1.7 and 1.85 eV. The ensemble spectrum of single isolated P3OT nanoparticles in a PVA matrix (Fig. 1d, solid line) shows analogous type of emission and peaks maxima as those of the nanoparticle water suspension. This reinforces the idea that the Type III emission is mainly associated with the aggregation of multiple chains, perhaps due to different polymer morphology for large aggregates than folded single chains.

Single molecule spectra

Figure 2 shows typical examples of single molecule emission spectra isolated at high dilution in an oxygen depleted polymer host to avoid photochemical artifacts. For more than 90% of the molecules investigated, the spectra did not exhibit any detectible time dependence of line shape or integrated intensity (i.e. due to photochemistry) during the irradiation period (~2 min), and the analysis was restricted to these stable molecules. It will be shown in a later section of this paper that due to the absence of oxygen in the samples, triplet quenching by oxygen is not a factor, and a significant population of triplets (as much as one per chain) are present during the spectroscopic measurements. Comparison of single molecule ensemble emission spectra in the presence and absence of oxygen (not shown), however, indicates that the presence of triplets does not significantly affects the shape of the emission spectrum of the singlet molecules, in analogy to SMS studies on MEH-PPV.

Figure 3a and b display the distributions of peak and mean emission energies for an ensemble of P3OT single molecules in PMMA. These distributions are much narrower than each single molecule spectrum itself demonstrating that the spectral broadening for each chain is much larger than that due to the molecule-to-molecule inhomogeneity. However, a detailed vibronic analysis of the individual spectra demonstrates that the major source of broadening is vibronic structure, followed by broadening due to the presence of more than one chromophore per chain, see below.

It is interesting to compare the distribution for P3OT to the analogous distributions for MEH-PPV (Fig. 3c and d), which have been previously reported. For MEH-PPV, two peaks are observed in the histograms, due qualitatively to

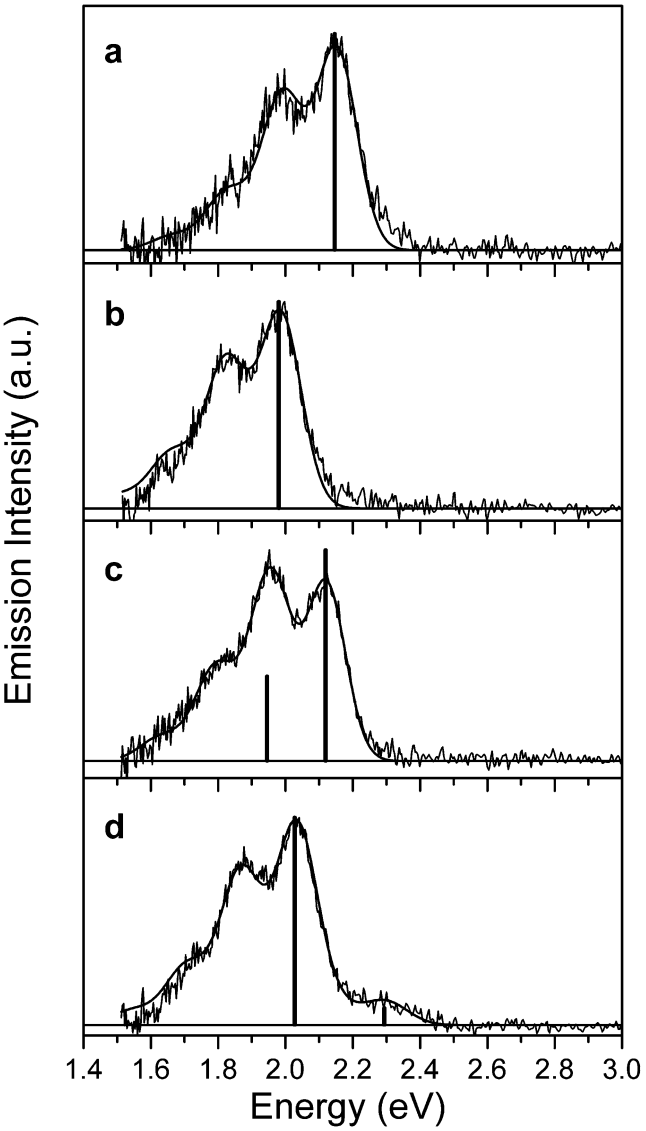

Fig. 2 (**a–d**) Typical emission spectra (λ_{exc}=488 nm) of single P3OT molecules. The *smooth line* corresponds to the fit to a Franck–Condon model as described in the text. The *bars* represent the amplitude and vibronic origin for each apparent chromophore used in the fitting

the presence or absence of low energy "red sites" sites in a specific polymer chain. For MEH-PPV single polymer chains with red sites, singlet excitons are efficiently trapped by the red sites. The efficiency of energy transfer from more plentiful blue sites to the red sites can approach unity for large molecular weight chains, and especially for the bulk polymer film [27, 28].

For P3OT, the distributions do not exhibit an obvious splitting due to blue and red sites, but rather a single broad distribution is observed. However, a detailed vibronic analysis which is presented below indicates that an analogous blue/red splitting exists for P3OT but it is masked by the dominance of the red form and a greater energy disorder of the individual red and blue forms for

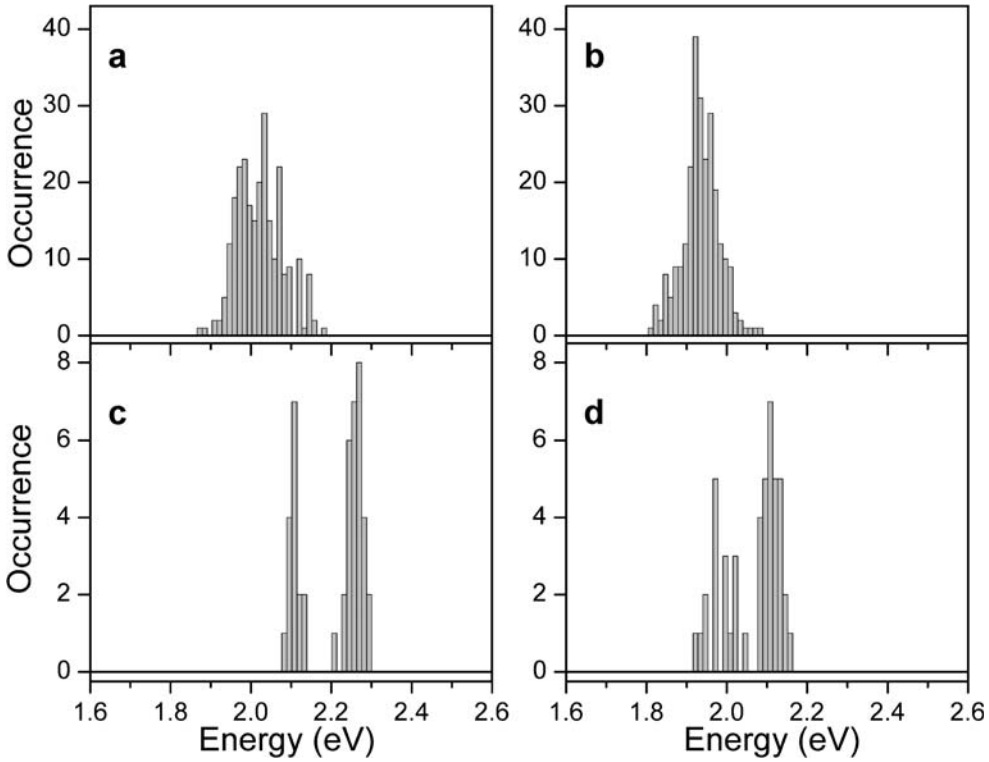

Fig. 3 Peak (**a**) and mean (**b**) wavelength distributions of single P3OT molecules emission spectra in PMMA matrix. Peak (**c**) and mean (**d**) wavelength distributions of single MEH-PPV molecules emission spectra in PMMA matrix

P3OT. The vibronic analysis of the SMS data was accomplished by fitting the individual spectra to a two mode, Franck–Condon model as described elsewhere [27]. Briefly, two C–C stretching modes with identical Huang–Rhys factors (S) and up to three vibrational quanta were considered. Each vibronic line was broadened by a Gaussian shape function with a common width, σ. In order to obtain a good fit of the model curves (shown as a smooth curve in panels a–d in Fig. 2) to the experimental data, it was necessary to use 1, 2, and (in few cases) even 3 distinct chromophores. The chromophores had distinct vibronic origins (E_0) but similar vibronic intensity patterns (given by S) that were typical of π–π* transitions. The bars in the spectra represent the amplitude and vibronic origin for each apparent chromophore used for the fitting.

Figure 2a and b show examples of SM spectra containing only one apparent chromophore. The spectrum in Fig. 2a contains a "blue" chromophore and the spectrum in Fig. 2b contains a "red" chromophore. Figure 2c shows an example of a SM spectrum in which two apparent chromophores were required for a successful fit of the experimental data. The spectrum in Fig. 2d shows a small high-energy peak that appears in rare occasions in the blue side of the SM spectra. In order to account for these peaks, chromophores with excess high energies were used in the fitting procedure. These features are tentatively assigned to the emission from high-energy chromophores that are temporarily populated during the energy transfer process in the single chains. Figure 4a portrays an ensemble average of experimental and fitted (smooth line) single molecule emission spectra. The chromophore energies resulting from the fits are represented by the stick plots under the spectra in Fig. 4. In the stick plots, a molecule can contribute 1, 2, or 3 "sticks" per chain due to the individual chromophores. The heights of the sticks reflect the relative intensity of each chromophore. The bar-plot inserts in Fig. 4, in contrast, represent the probability distributions of lowest transition energies, E_0' (one per molecule), within the respective ensemble or sub-ensemble. This latter data has higher resolution that the peak and mean emission maxima distributions shown in Fig. 3 due to the fitting of the individual chromophores. While the ensemble E_0' data does not exhibit a resolved bimodal distribution, a qualitative indication of a bimodal energy distribution (red/blue) is apparent in the sub-ensemble spectra, as shown in Fig. 4b and c, using the lowest energy E_0' as a sorting criteria. The molecules selected for the sub-ensemble are indicated by the filled bars in the inserts.

The molecules on the low energy side of the E_0' distribution are well-fit almost exclusively by individual red chromophores with E_0 energies ranging from 1.91 to 2.01 eV. The blue sub-ensemble, is well-fit by a combination of "red" and "blue" chromophores having E_0 energies in the 1.94–1.99 and 2.15–2.08 eV ranges, respectively. The presence of two emitting chromophores per molecules (i.e. dual emission) is further evidence for a bimodal energy distribution of red and blue chromophores and is analogous to that previously observed for MEH-PPV. Thus, various

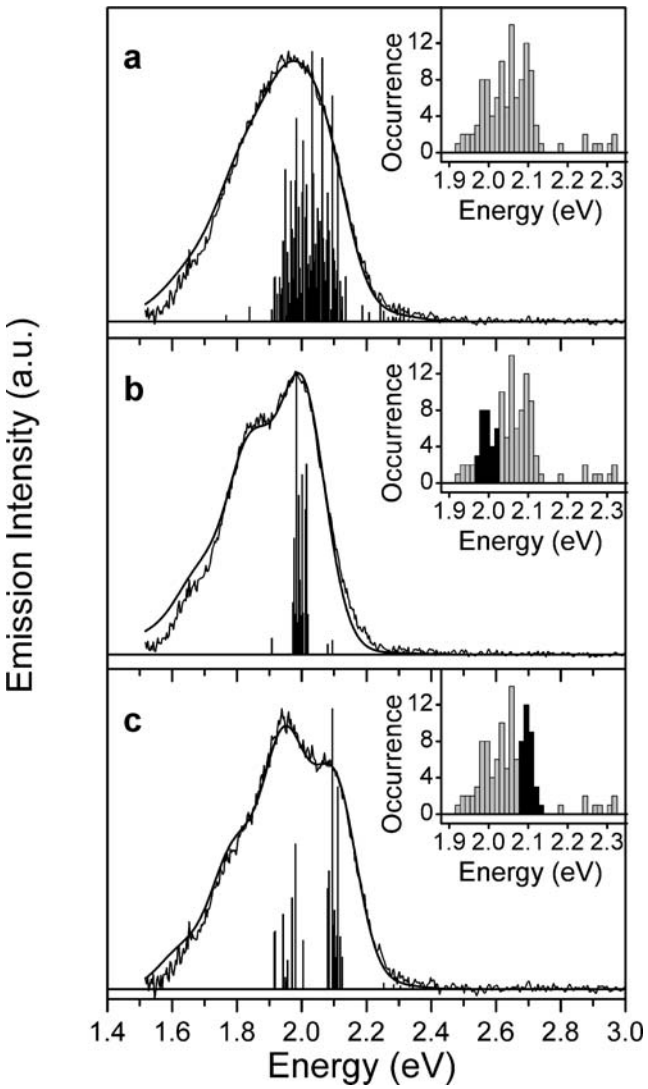

Fig. 4 Experimental and calculated (*smooth line*) ensemble (**a**) and sub-ensemble (**b** and **c**) spectra of P3OT in PMMA matrix. The *bars* represent the energies and amplitudes of the 0,0 transitions from calculated fits. The *inserts* show the histogram corresponding 0,0 transition energies for the lowest energy chromophores in each spectrum. Panel (**a**) shows the total ensemble spectrum. Panels (**b**) and (**c**) show *red* and *blue* sub-ensembles constructed by adding up single molecule spectra with peak wavelengths in the 1.97–2.02 and 2.08–2.13 eV ranges, respectively. The *solid black bars* in the histograms for the corresponding inserts indicate the selected ranges

types of evidence suggests that P3OT does in fact possess two sub-types of Type II chromophores, due to red and blue sites, which we designate, respectively Type IIA and IIB.

In light of this observation, it is interesting to reexamine the ensemble spectra shown in Fig. 1. The shift between the emission in a good solvent and in the PMMA solution can now be interpreted as being due to an increase in the number of red sites per polymer chain due to polymer collapse in the PMMA environment. A similar observation has been made for MEH-PPV [29].

SMS modulation spectroscopy of P3OT

It was recently shown for MEH-PPV and F8BT single polymer chains in oxygen free environments that triplet excitons can be present at significant concentrations in the polymer chains under moderate to high excitation conditions. Since triplet excitons are efficient quenchers of singlet excitons by energy transfer, the steady state emission intensity of single polymer chains can be significantly

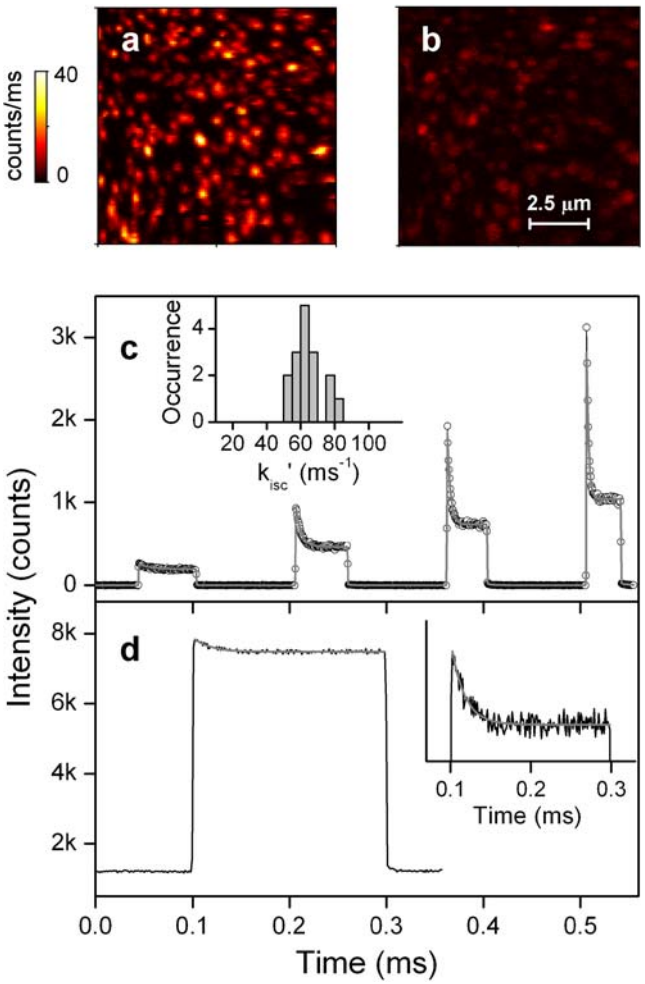

Fig. 5 (**a** and **b**) Typical confocal fluorescence images of P3OT single molecules in PMMA matrix. Both images were obtained from the same sample under the same excitation power (44 W/cm^2 at 488 nm). Image (**a**) is of a region not covered by the *gold* layer and exposed to atmospheric oxygen, image (**b**) is of a *gold coated* region. (**c**) Typical excitation intensity modulation data for single P3OT molecules (*data points*) and the corresponding fit to the kinetic model (*solid line*). The intensities of the four sequential excitation pulses (λ_{exc}=488 nm) are 6, 21, 44, and 75 W/cm^2, from *left* to *right*, respectively. The *insert* shows a histogram of the reverse intersystem crossing rates obtained from the fitting of 15 individual molecules. (**d**) Average low power intensity modulation data for five P3OT molecules. The average intensity during the excitation window is 0.4 W/cm^2. The *insert* shows an enlarged view of the *top part* of the excitation window, the *grey smooth line* represents a single-exponential fit to the data with a lifetime of 17±1.5 μs

quenched by the presence of triplets. One consequence of this effect is shown qualitatively in Fig. 5a and b, which correspond to confocal images of a sample of P3OT molecules in PMMA matrix containing high and low concentrations of oxygen respectively. The images clearly show that the emission of single molecules at saturated oxygen conditions is significantly higher than that at low oxygen concentrations. The low intensity in the oxygen-depleted sample is due to the buildup of triplet states which are efficient singlet quenchers, while in the oxygenated samples triplets are quickly quenched by oxygen-induced intersystem crossing.

Figure 5c portrays the SMS fluorescence intensity of a typical single molecule recorded while modulating the laser intensity in the form of four laser pulses of intensities, 6, 21, 44, and 75 W/cm^2. The data were synchronously averaged for approximately 10^5 cycles of the pulse sequence. The shape of the fluorescence response to each pulse has been previously described for MEH-PPV to be due to an initial drop in intensity resulting from a build-up of triplet population during the excitation pulses [24]. The off period between pulses is sufficiently long to ensure that the triplet population completely relaxes between pulses. It has been shown that data of this type can be analyzed (fitted) to extract parameters such as the rate of reverse intersystem crossing, the probability of quenching singlet excitons by triplet excitons, and the cross section for absorption [24, 28].

The basic form of the data, i.e. a single exponential decay to a steady-state intensity, is indicative of rapid triplet-triplet exciton annihilation. Due to this process, no more than one triplet exciton per chain is present on average during the intensity modulation cycle. At high excitation power, the rapid exponential decay at the beginning of each pulse is primarily due to the rate of creating triplet excitons, i.e. the product of the excitation rate and the quantum yield for intersystem crossing. At low excitation power the time scale for establishing the fluorescence steady state is simply the inverse of the reverse intersystem crossing rate constant (i.e. the triplet lifetime). Thus, this excitation power regime can be used to measure the reverse intersystem crossing rate constant for single polymer chains.

Figure 5c shows the typical excitation intensity modulation data for single P3OT molecules and the corresponding best-fit of the previously described kinetic model to the data. The excellent agreement between the experimental data and the best-fit model curves supports the application of this kinetic model to analyze exciton dynamics in P3OT. The insert shows a histogram of the reverse intersystem crossing rates (k_{isc}') with a mean value of 62 ms^{-1} (σ=9 ms^{-1}) obtained from the fitting of 15 individual molecules. The corresponding triplet lifetime of 16 μs is in good agreement with the reported value in benzene solution (21 μs) [40]. This result not only further validates the application of the kinetic model for P3OT but also confirms the assignment of the triplet exciton state as significant quencher of singlet excitons in SMS experiments.

Figure 5d shows the results of the low power intensity modulation experiments. In order to get a reasonable signal to noise ratio, the fluorescence intensity traces from five individual molecules were averaged. At the power level used in these experiments the kinetic population of states model predicts that the observed intensity decay is essentially equal to the triplet lifetime. This prediction is confirmed by fitting the data to an exponential function which yields a lifetime of 17±1.5 μs in excellent agreement with the mean triplet lifetime observed at higher powers (16 μs).

Conclusions and summary

In conclusion we have investigated for the first time the single molecule spectroscopy of the conjugated polymer P3OT. The results show that single P3OT chains isolated in an inert polymer do not show emission from the lowest energy aggregated form of P3OT associated to distinct crystalline phases. The lack of aggregate fluorescence allowed us to study in detail the emission in the 1.9–2.2 eV range and it was observed that in fact this band is split into low (red) and high (blue) energy forms. The presence of this dual emission was rationalized in terms of chain packing effects that create high and low energy chromophores in analogy to the red and blue sites recently reported for MEH-PPV. In the case of P3OT, however, the dual emission is masked in the peak/mean wavelength histograms by the dominance of the red form and a greater energy disorder of the individual red and blue forms.

In addition to the analysis of single molecule spectra we investigated the dynamics of singlet–triplet interactions in P3OT by using the recently developed single molecule intensity modulation technique. The results show that triplet excitons are highly efficient fluorescence quenchers for P3OT, strongly quenching the fluorescence of the P3OT under even relatively low excitation intensities. The good agreement between the P3OT triplet lifetime obtained in our experiments and the reported value in the literature strongly supports the assignment of the triplet state as the main quencher of singlet excitons in conjugated polymers.

We conclude that single molecule spectroscopy of P3OT is highly analogous in many aspects to that of MEH-PPV and other conjugated polymers. This observation highlights the ability of SMS techniques to study this important class of organic electronic materials.

Acknowledgements We gratefully acknowledge the Basic Energy Sciences Program of the Department of Energy and the Robert A. Welch Foundation for support of this research. We thank Brent C. Norris for making the nanoparticle samples that were studied in this paper.

References

1. Bolognesi A, Giacometti Schieroni A, Botta C, Marinelli M, Mendichi R, Rolandi R, Relini A, Inganas O, Theandher M (2003) High photoluminescence efficiency in substituted polythiophene aggregates. Synth Met 139(2):303–310
2. Ahn S-H, Czae M-Z, Kim E-R, Lee H, Han S-H, Noh J, Hara M (2001) Synthesis and characterization of soluble polythiophene derivatives containing electron-transporting moiety. Macromolecules 34(8):2522–2527
3. Bolognesi A, Bajo G, Paloheimo J, Ostergaard T, Stubb H (1997) Polarized electroluminescence from an oriented poly(3-alkylthiophene) Langmuir–Blodgett structure. Adv Mater (Weinheim, Germany) 9(2):121–124
4. Barta P, Salaneck WR, Zagorska M, Pron A, Niziol S (1996) Electroluminescence of regioregular poly(alkylthiophenes). Adv Mater Opt Electron 6(5, 6):406–408
5. Uchida M, Ohmori Y, Morishima C, Yoshino K (1993) Visible and blue electroluminescent diodes utilizing poly(3-alkylthiophenes) and poly(alkylfluorenes). Synth Met 57(1):4168–4173
6. Sirringhaus H, Tessler N, Thomas DS, Brown PJ, Friend RH (1999) High-mobility conjugated polymer field-effect transistors. Adv Solid State Phys 39:101–110
7. Sirringhaus H, Tessler N, Friend RH (1999) Integrated, high-mobility polymer field-effect transistors driving polymer light-emitting diodes. Synth Met 102(1–3):857–860
8. Li G, Shrotriya V, Huang J, Yao Y, Moriarty T, Emery K, Yang Y (2005) High-efficiency solution processable polymer photovoltaic cells by self-organization of polymer blends. Nat Mater 4(11):864–868
9. Yang X, Loos J, Veenstra SC, Verhees WJH, Wienk MM, Kroon JM, Michels MAJ, Janssen RAJ (2005) Nanoscale morphology of high-performance polymer solar cells. Nano Lett 5(4): 579–583
10. Coakley KM, Liu Y, McGehee MD, Frindell KL, Stucky GD (2003) Infiltrating semiconducting polymers into self-assembled mesoporous titania films for photovoltaic applications. Adv Funct Mater 13(4):301–306
11. Huynh WU, Dittmer JJ, Alivisatos AP (2002) Hybrid nanorod-polymer solar cells. Science (Washington, DC, United States) 295(5564):2425–2427
12. Yang C, Orfino FP, Holdcroft S (1996) A phenomenological model for predicting thermochromism of regioregular and nonregioregular poly(3-alkylthiophenes). Macromolecules 29(20):6510–6517
13. Xu B, Holdcroft S (1993) Molecular control of luminescence from poly(3-hexylthiophenes). Macromolecules 26(17): 4457–4460
14. Sundberg M, Inganaes O, Stafstroem S, Gustafsson G, Sjoegren B (1989) Optical absorption of poly(3-alkylthiophenes) at low temperatures. Solid State Commun 71(6):435–439
15. Sakurai K, Tachibana H, Shiga N, Terakura C, Matsumoto M, Tokura Y (1997) Experimental determination of excitonic structure in polythiophene. Phys Rev, B Condens Matter 56(15): 9552–9556
16. Rumbles G, Samuel IDW, Magnani L, Murray KA, DeMello AJ, Crystall B, Moratti SC, Stone BM, Holmes AB et al (1996) Chromism and luminescence in regioregular poly(3-dodecylthiophene). Synth Met 76(1–3):47–51
17. Mao H, Xu B, Holdcroft S (1993) Synthesis and structure–property relationships of regioirregular poly(3-hexylthiophenes). Macromolecules 26(5):1163–1169
18. Luzzati S, Elmino P, Bolognesi A (1996) Luminescence excitation spectroscopy of highly oriented poly(3-octylthiophene)-polyethylene blends. Synth Met 76(1–3):23–26
19. Kanemoto K, Shishido M, Sudo T, Akai I, Karasawa T, Agari Y (2005) Effect of the dilution in polypropylene on photophysical properties of poly(3-alkylthiophenes). Synth Met 155(1):162–167
20. Chen TA, Wu XM, Rieke RD (1995) Regiocontrolled synthesis of Poly(3-Alkylthiophenes) mediated by Rieke Zinc—their characterization and solid-state properties. J Am Chem Soc 117(1): 233–244
21. Bolognesi A, Porzio W, Provasoli A, Botta C, Comotti A, Sozzani P, Simonutti R (2001) Structural and thermal behavior of poly(3-octylthiophene): a DSC, C-13 MAS NMR, XRD, photoluminescence, and Raman scattering study. Macromol Chem Phys 202(12):2586–2591
22. Yamamoto T, Komarudin D, Maruyama T, Arai M, Lee B-L, Suganuma H, Asakawa N, Inoue Y, Kubota K, Sasaki S, Fukuda T, Matsuda H (1998) Extensive studies on p-stacking of poly(3-alkylthiophene-2,5-diyl)s and poly(4-alkylthiazole-2,5-diyl)s by optical spectroscopy, NMR analysis, light scattering analysis, and x-ray crystallography. J Am Chem Soc 120(9): 2047–2058
23. Hu DH, Yu J, Wong K, Bagchi B, Rossky PJ, Barbara PF (2000) Collapse of stiff conjugated polymers with chemical defects into ordered, cylindrical conformations. Nature 405(6790): 1030–1033
24. Gesquiere AJ, Lee YJ, Yu J, Barbara PF (2005) Single molecule modulation spectroscopy of conjugated polymers. J Phys Chem B 109(25):12366–12371
25. Yu J, Lammi R, Gesquiere AJ, Barbara PF (2005) Singlet–triplet and triplet–triplet interactions in conjugated polymer single molecules. J Phys Chem B 109(20):10025–10034
26. Barbara PF, Gesquiere AJ, Park SJ, Lee YJ (2005) Single-molecule spectroscopy of conjugated polymers. Acc Chem Res 38(7):602–610
27. Kim DY, Grey JK, Barbara PF (2006) A detailed single molecule spectroscopy study of the vibronic states and energy transfer pathways of the conjugated polymer MEH-PPV. Synth Met 156(2–4):336–345
28. Lee YJ, Kim DY, Grey JK, Barbara PF (2005) Variable temperature single-molecule dynamics of MEH-PPV. Chemphyschem 6(11):2404–2409
29. Yu J, Hu DH, Barbara PF (2000) Unmasking electronic energy transfer of conjugated polymers by suppression of O-2 quenching. Science 289(5483):1327–1330
30. Szymanski C, Wu C, Hooper J, Salazar MA, Perdomo A, Dukes A, McNeill J (2005) Single molecule nanoparticles of the conjugated polymer MEH-PPV, preparation and characterization by near-field scanning optical microscopy. J Phys Chem B 109(18):8543–8546
31. Grey JK, Kim DY, Norris BC, Miller WL, Barbara PF (2006) Size dependent spectroscopic properties of conjugated polymer nanoparticles. J Phys Chem B 110(51):25568–25572
32. Palacios RE, Fan F-RF, Bard AJ, Barbara PF (2007) Spectroelectrochemistry studies of the charging and discharging of single conjugated-polymer nanoparticles. Nat Mater (submitted)
33. Hu DH, Yu J, Barbara PF (1999) Single-molecule spectroscopy

of the conjugated polymer MEH-PPV. J Am Chem Soc 121(29):6936–6937
34. Havinga EE, Rotte I, Meijer EW, Tenhoeve W, Wynberg H (1991) Spectra nd electrical-properties of soluble partially alkyl-substituted oligomers of thiophene up to 11 rings. Synth Met 41(1–2):473–478
35. Tenhoeve W, Wynberg H, Havinga EE, Meijer EW (1991) Substituted 2,2′-5′,2″-5″, 2(′X3)-5(′X3), 2(′X4)-5(′X4), 2(′X5)-5(′X5), 2(′X6)-5(′X6), 2(′X7)-5(′X7), 2(′X8)-5(′X8), 2(′X9)-5(′X9), 2(′X10)-undecithiophenes—the longest characterized Oligothiophenes. J Am Chem Soc 113(15):5887–5889
36. Nakanishi H, Sumi N, Aso Y, Otsubo T (1998) Synthesis and properties of the longest oligothiophenes: the icosamer and heptacosamer. J Org Chem 63(24):8632–8633
37. Sumi N, Nakanishi H, Ueno S, Takimiya K, Aso Y, Otsubo T (2001) Synthesis and properties of a series of the longest oligothiophenes up to the 48-mer. Bull Chem Soc Jpn 74 (5):979–988
38. Nakanishi H, Sumi N, Ueno S, Takimiya K, Aso Y, Otsubo T, Komaguchi K, Shiotani M, Ohta N (2001) Spectral properties of the longest oligothiophenes in the oxidation states. Synth Met 119(1–3):413–414
39. Furukawa Y, Akimoto M, Harada I (1987) Vibrational key bands and electrical conductivity of polythiophene. Synth Met 18(1–3):151–156
40. Monkman AP, Burrows HD, Hartwell LJ, Horsburgh LE, Hamblett I, Navaratnam S (2001) Triplet energies of pi-conjugated polymers. Phys Rev Lett 86(7):1358–1361
41. McCullough RD, Lowe RD, Jayaraman M, Anderson DL (1993) Design, synthesis, and control of conducting polymer architectures: structurally homogeneous poly(3-alkylthiophenes). J Org Chem 58(4):904–912